

Comparison of Non-Detection Zone of Frequency Drift Anti-islanding with Closed-loop Power Controlled Distributed Generators

Byeong-Heon Kim and Seung-Ki Sul
Dept. of Electrical and Computer Engineering
Seoul National University
Seoul, Republic of Korea
heon13@snu.ac.kr

Abstract— In this paper, the Non Detection Zones (NDZs) of frequency drift anti-islanding were compared according to the structure of positive feedback loop for closed-loop power controlled Distributed Generators (DGs). It was reported that the NDZ of frequency drift anti-islanding is enlarged with closed-loop based constant power controller. On the other hand, some research gives the functionality of the frequency drift anti-islanding even with the closed-loop power controller. If the principle of frequency drift is carefully considered, the positive feedback loop should be modified to maintain the performance of the conventional frequency drift anti-islanding when the cascade outer (power control) loop is constructed. And the NDZ of modified loop would not be degraded by the outer loop. In this paper, the rationale of the modification of the closed-loop is discussed. And, it is shown that the modified feedback loop doesn't degrade the performance of the frequency drift anti-islanding with the closed-loop power controller. The performance of modification is verified by computer simulations and hardware experiments.

Index Terms— Distributed generator, anti-islanding, frequency drift method, closed-loop power controller.

I. INTRODUCTION

The islanding is defined as a condition where a portion of the utility system, which is energized by one or more local electric power systems through the associated point of common coupling (PCC), is electrically separated from the remainder of utility system [1], [2]. The anti-islanding is the method to detect islanding condition. Because the islanding can be a severe threat to the grid operation, anti-islanding functionality is mandatory feature for distributed generators (DGs) [1]-[3].

The anti-islanding inside DG's software implementation could be divided into passive and active methods. Among active methods, the frequency drift method (FDM) based on positive feedback between reactive power and grid frequency is one of the most popular methods and equipped in many grid connected inverters [4]. The Active Frequency Drift (AFD), Sandia Frequency Shift (SFS) or Slip-Mode frequency Shift

(SMS) are the representative algorithm for FDM, which are developed originally for single phase photovoltaic (PV) applications. These methods control the phase of inverter output current, which is modulated by function of grid frequency. Because the frequency is drift away during islanding due to the positive feedback, the FDMs can detect islanding by triggering Over/Under Frequency (OUF) relay [5], which is the basic requirement for grid connected inverter [1]-[3]. The Non-Detection Zone (NDZ) for FDMs, which is the performance index for anti-islanding, is commonly depicted on load plane of quality factor and resonant frequency of islanding load [6]. To extend these algorithms to three phase DG application, simple rotation of the current reference vector is applied.

However, in the case of DG control systems equipped with closed-loop constant power controller, it had been known that these algorithms would not work well and mentioned that the NDZs would be enlarged [6]. On the other hand, some research had shown the possibility of the frequency drift even with the closed-loop power controller [7], [8]. As far as authors know, there have been no reports for discussing why these different results occur.

In this paper, the NDZs of frequency drift anti-islanding algorithm for DGs equipped with the closed-loop power controller are analyzed. At first, the fundamental characteristics of frequency positive feedback are discussed under the consideration that not the phase of current reference but the reactive component of the reference has to be modulated. The contradiction of previous reports comes from the misunderstanding of positive feedback and this misconception results in inadequate construction of feedback loop under outer power control loop.

With this consideration, the positive feedback loop on power controlled DGs is suggested to achieve a designed FDM performance. With the conventional FDM, modified SFS, the NDZs with different positive feedback loops are compared. These are verified by computer simulations and hardware experiment.

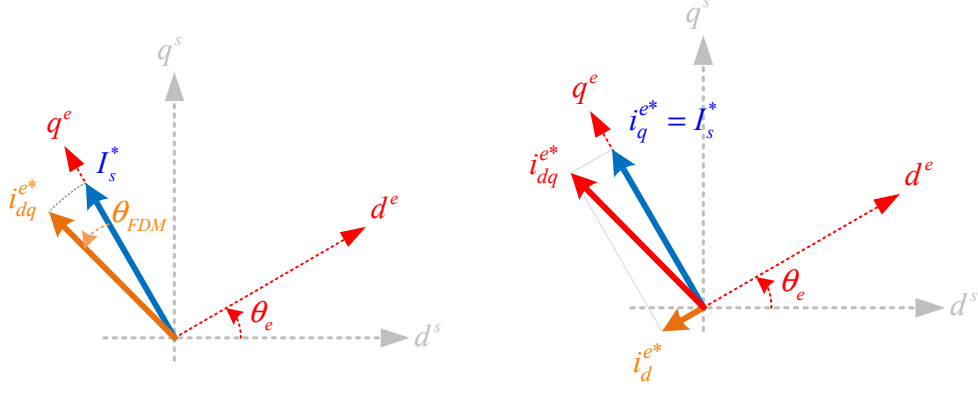


Figure 1. Implementation of frequency drift anti-islanding in three phase system

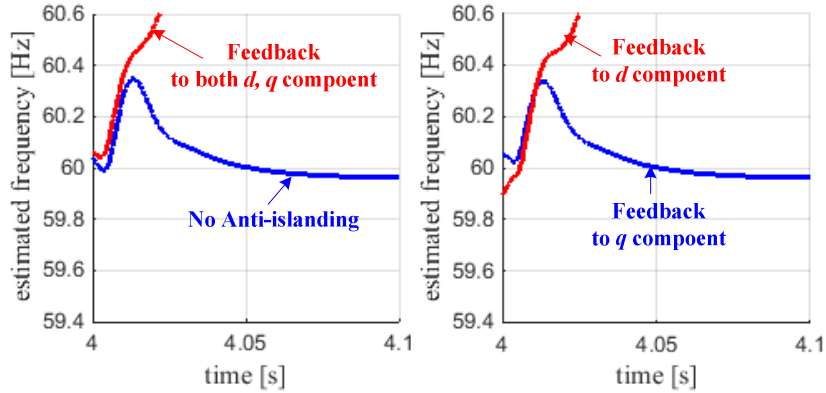


Figure 2. Islanding test with variety feedback

II. DISCUSSION FOR EXTENSION OF FREQUENCY DRIFT ANTI-ISLANDING TO THREE PHASE DGs

In the FDMs, the estimated grid frequency is fed back to the phase of current reference, and this results in frequency drift after islanding. In order to extend these algorithms to three-phase DGs, frequency feedback would be applied to each phase of three phase current references. This simple extension leads to the rotation of the current reference vector as shown in Fig. 1 (a) [6]. The modified current references, which are represented in synchronous reference frame and complex vector, can be obtained by (1). In this paper, the q -axis current is defined as active power component and is imaginary number in complex vector. If the q -axis current has positive value, DG supplies active power to the grid. For the d -axis current, capacitive current has positive value and inductive current has negative value.

$$i_{dqs}^{e*} = \exp(-j\theta_{FDM}) j I_s^* \quad (1)$$

where, θ_{FDM} represents the feedback component for frequency drift and is function of grid frequency. And I_s^* represents the magnitude of original current reference produced by outer loop or reference generator. And, i_{dqs}^{e*} is the complex vector of modified current reference. The real value of complex vector means the d -axis component.

However, the reactive power mismatch is the main reason of the frequency drift after islanding as discussed in [7] or [8]. Only reactive component of current reference in (1) would drift frequency to outward of normal frequency range; the active current, real value in (1), has nothing to do with the frequency drift. In result, only reactive component should be modulated as a positive feedback as shown in Fig. 1 (b).

The equations (2) and (3) represent the each component of current reference to apply frequency drift anti-islanding using the injection of reactive component only. The approximation is valid under normal frequency range. Under assumption that it is designed to inject only reactive component for FDM, the active current is set to magnitude of original current reference (I_s^*) instead of the imaginary value of the equation (1).

$$i_{qs}^{e*} = I_s^* \quad (2)$$

$$i_{ds}^{e*} = -\sin \theta_{FDM} \times I_s^* \approx -\theta_{FDM} \times I_s^* \triangleq \Delta i_{ds}^{e*} \quad (3)$$

In Fig. 2, the simulation results under constant current control without any outer power control loop is shown. Among various FDM, the modified SFS in [9] is adopted and the feedback component can be calculated by (4)

$$\Delta i_{ds}^{e*} = K_q(f - f_0) \times I_s^* \quad (4)$$

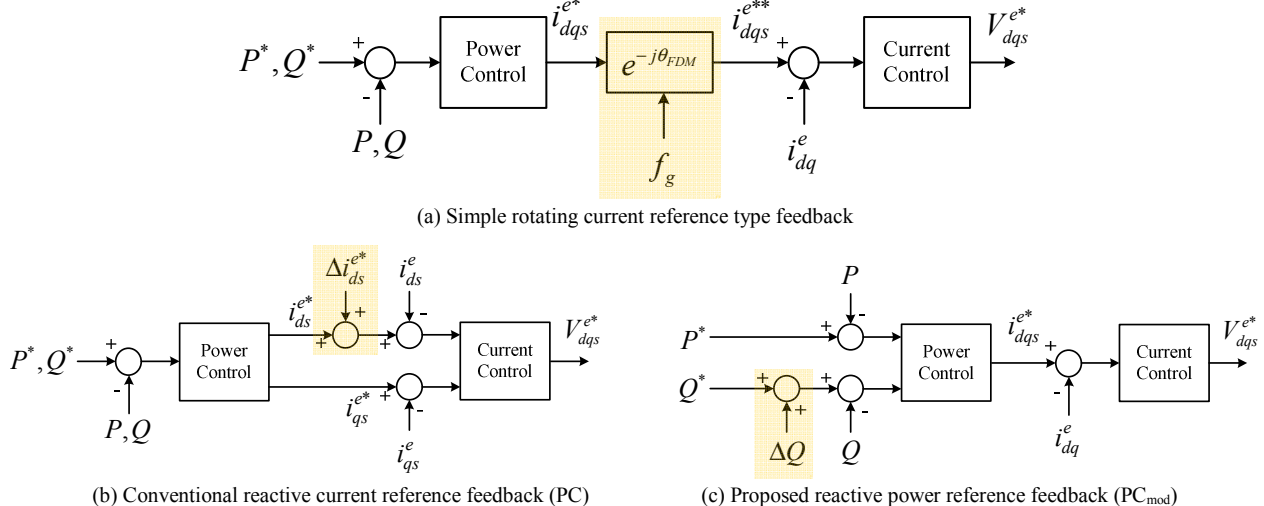


Figure 3. Positive feedback loops

where, K_q is the positive feedback gain and has negative value.

In the simulation at Fig. 2, the islanding occurs at time point, 4s. When the feedback is applied to the active component, islanding cannot be detected and show similar dynamics to the result without anti-islanding. And, it can be seen that only imaginary feedback term in (1) is not working for frequency drift. The feedback term with only reactive component show similar dynamics with the whole rotation of current vector after islanding. This reactive component feedback enables to detect islanding by drifting away the grid frequency to abnormal range.

The above discussion and the simulation results reveal that not a phase of current, but the reactive power component can make drift of the grid frequency after islanding. Using this consideration, the effective positive feedback loop can be implemented under the closed-loop constant power controller.

III. FREQUENCY POSITIVE FEEDBACK LOOP UNDER CLOSED-LOOP POWER CONTROL

In the Fig. 3, various positive feedback loops under the closed-loop power controlled DGs are depicted. As mentioned before, the simple rotation of current vector (Fig. 3 (a)) and the reactive current injection (Fig. 3 (b)), which is implemented with the reactive current feedback, show similar dynamics without the outer power control loop as shown in Fig. 2. In the followed discussion, the only reactive current feedback is considered as the conventional feedback loop.

However, the conventional reactive power current injection method doesn't work well under closed-loop power controlled DGs, because the outer loop makes output current follow the reactive power reference. This output current cancels the component intentionally inserted for islanding detection. After islanding, the reactive power of DG eventually follows the reactive power reference which might equal to be null. Such mechanism, which controls reactive

power of DG, degrades the performance of frequency drift. And, the NDZ would be enlarged.

To induce frequency drift effectively after islanding, the reactive power of DGs should be directly modulated. The proposed positive feedback loop in Fig. 3 (c) could be a candidate. This structure directly modulates the reactive power regardless of outer power control loop in the islanded condition. The equivalent feedback component of Fig. 3 (c) could be calculated as follows.

$$\Delta Q = -\sin \theta_{FDM} \times P_{DG} \approx -\theta_{FDM} \times P_{DG} \quad (5)$$

where, P_{DG} represents the active power reference or that of DG.

By (5), without the loss of generality, all of FDMs can be effectively applied to outer power control loop.

IV. NON DETECTION ZONE

As discussed in the section II, the relationship between the reactive power of DG and that of load determines the NDZ. The grid frequency would be moved to abnormal frequency range, or be converged to normal frequency range. In the former case, the OUF relay would be triggered and the islanding could be detected. The latter case, though, the grid frequency remains in normal operation range and the inverter continuously feeds energy to the grid. That is, by the grid frequency in steady state, the NDZ of FDM would be determined.

To obtain NDZ on load plane, the convergent frequency should be calculated. The convergent frequency after islanding is the crossover point of reactive power curve of DG and of islanding load. The equation of reactive power curve of DG can be represented by (5).

If the parallel RLC load is assumed, under islanding condition, the load has reactive power curve as (6).

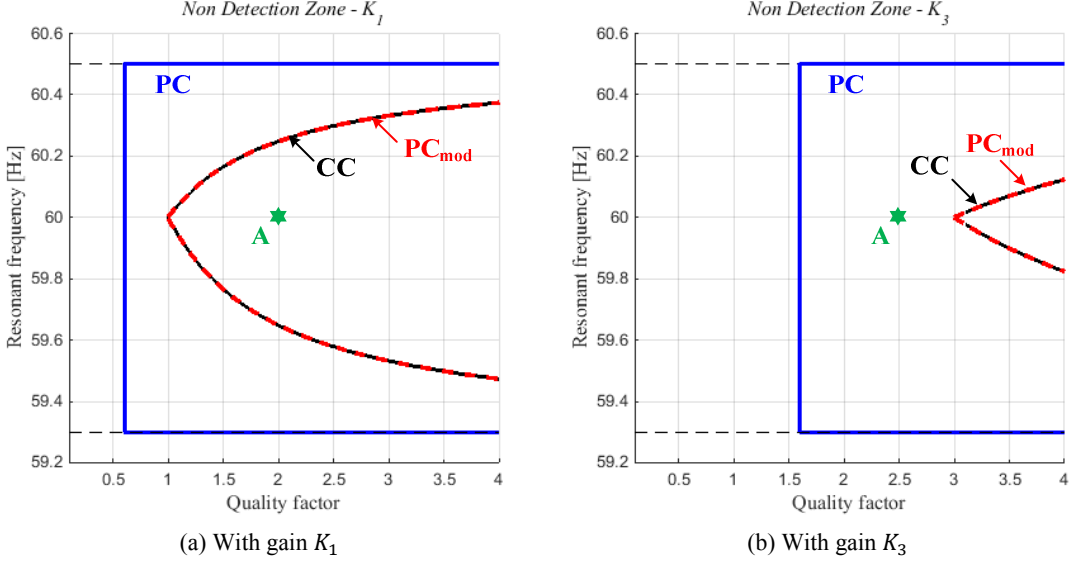


Figure 4: Non-Detection Zone

$$Q_{load} = P_{DG} Q_f (f_0 f_{is}^{-1} - f_{is} f_0^{-1}) \quad (6)$$

where, Q_f is the quality factor of islanding load and f_0 is the resonant frequency of the load [1]. f_{is} is the grid frequency at the point of common coupling (PCC) after islanding.

Because this could be linearized around operation frequency, (6) can be changed to (7) [7].

$$Q_{load} \approx -2P_{DG} Q_f f_0^{-1} (f_g - f_0) \quad (7)$$

Based on (5) and (7), the crossover point can be calculated as (8).

$$f_{cross} = 0.5Q_f^{-1} f_0 \theta_{FDM} (f_{cross}) + f_0 \quad (8)$$

Because θ_{FDM} is the function of crossover point, the (8) has implicit form. If the θ_{FDM} is linearized, (8) could be expressed explicitly.

In the case of the constant current control or the power control with the proposed positive feedback loop, this point f_{cross} represents the steady state grid frequency after islanding. Similar to phase criterion, the two border lines, the curve obtained by lower and upper limit of normal frequency in load plane, construct NDZ plot in the steady-state [6].

However, in the case of conventional feedback loop to reactive current, because of the existence of the outer loop, the border line of NDZ couldn't be predicted by (8). The NDZ of the conventional feedback loop can be obtained by computer simulation or solution of small signal model derived in [6].

In Fig. 4, the NDZs according to the structure of feedback loop are shown. The normal operation range of the grid frequency is set to 59.3 to 60.5 Hz. The NDZ of constant current control without the outer power control loop (CC) is also plotted for the comparison. According to the design rule in [7], the feedback gains are selected. Each gains K_1 , and K_3

was designed to detect islanding load which has quality factor 1 and 3, respectively.

For the closed-loop power controller, although same algorithm was adopted, the NDZ of the proposed positive feedback to power reference, denoted as PC_{mod} in the figure, is much smaller than that of the conventional current reference feedback as PC in the figure. Compared to the current controlled DGs, the designed performance could be kept with the proposed reactive power injection method with the simple modification of the loop. As the gains are set to detect load which has quality factor 1 and 3 respectively, the load with quality factor below designed value would be always detected by the proposed feedback loop. But the conventional loop cannot show frequency drift at the designed load condition.

For example, the load condition 'A' in the Fig. 4 cannot be detected by the feedback gain K_1 . However, with K_3 , the islanding shall be detected according to the feedback loop. The simulation result of Fig. 2 shows the islanding detection performance with K_3 , where the outer power control loop is omitted.

V. EXPERIMENTAL RESULTS

By the experiment, the analysis for NDZs is also verified. The islanding load contains three phase passive components (R, L, C). The quality factor of islanding load in experiment was set to 2; The 'A' point in Fig. 4 represents this load condition in the experiments. The OUF relay was set to be triggered under 55 Hz and over 65 Hz for simplicity. The experimental conditions are arranged on Table I.

As shown in Fig. 5, the conventional reactive current feedforward algorithm cannot detect the islanding even with gain K_3 as expected by NDZ analysis. With both gains, the grid frequency after islanding converges to the resonant frequency of the load. While, through the proposed algorithm with gain K_3 , the islanding is detected within 1.3s as shown in Fig. 6, which meets international standard. If the normal frequency zone shrinks from 55 Hz ~ 65 Hz to 59.3 Hz ~ 60.5

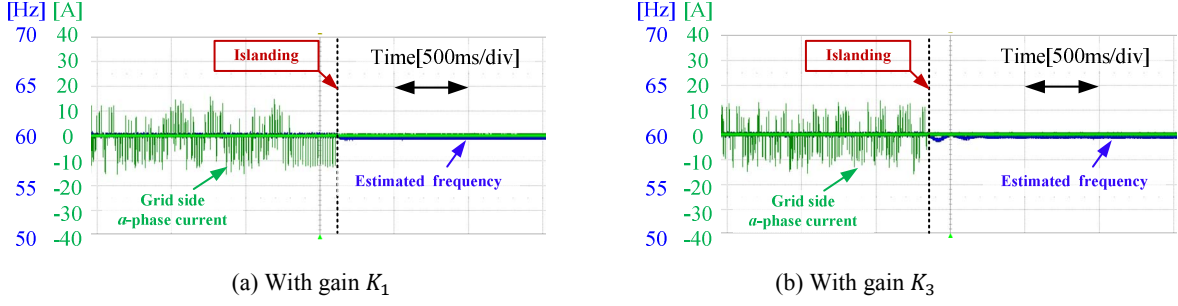


Figure 5: Experimental results – with reactive current reference feedback

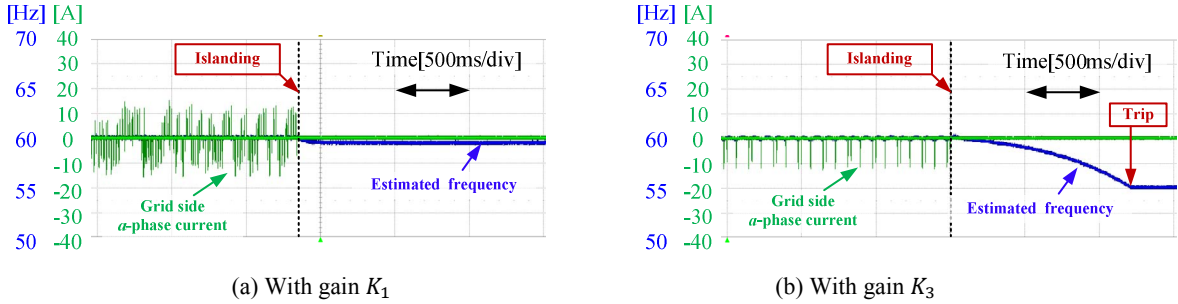


Figure 6: Experimental results – with the proposed reactive power reference feedback

Hz, the detection time would be less than a few hundreds milliseconds. If the feedback gain is carefully tuned, the detection time could be reduced further.

The experimental results reveal that the performance degradation for islanding detection would not come from the construction of outer loop, but from the inadequate positive feedback loop.

VI. CONCLUSIONS

In this paper, the fundamental principle of frequency drift anti-islanding has been reviewed, and the effective positive feedback loop to detect islanding for DG equipped with closed-loop power controller has been proposed. The conventional understanding for frequency drift based on phase criterion was not sufficient to make effective positive feedback loop in the presence of outer power controller. By considering the reactive power relation with outer loop, the positive feedback should be directly applied to reactive power reference. By positive feedback to reactive power component, the frequency drift anti-islanding has overcome the degradation of NDZ for DGs even equipped with the closed-loop power controller. The detection performance of the proposed modified closed loop becomes similar to that of the current controlled DGs without the outer power control loop. The islanding detection performances are compared in view point of NDZ obtained by computer simulations. The NDZ analysis is also verified by the experimental results. By the modified feedback loop, it is possible that the islanding detection time fulfills the requirements of the international standards.

TABLE I. PARAMETERS IN EXPERIMENT

Nominal grid voltage	220 V	
Nominal grid frequency	60Hz	
Rated power of system	5 kW	
Islanding load ($Q_f = 2$)	R	9.68 Ω
	L	12.8 mH
	C	580 μF

REFERENCES

- [1] IEEE Recommended Practice for Utility Interface of Photovoltaic (PV) Systems, IEEE Standard 929-2000.
- [2] IEEE Standard for Interconnecting Distributed Resources with Electric Power Systems, IEEE Standard 1547-2003 (R2008).
- [3] Inverters, Converters, Controllers and Interconnection System Equipment for Use with Distributed Energy Resources, UL 1741-2005.
- [4] B.-H. Kim and S.-K. Sul, "Anti-islanding accelerated by grid unbalance component," in 9th International Conf. on Power Electron. and ECCE Asia (ICPE-ECCE Asia 2015), 2015, pp. 1268-1275.
- [5] L. A. Lopes and H. Sun, "Performance assessment of active frequency drifting islanding detection methods," *IEEE Trans. Energy Conversion*, vol. 21, pp. 171-180, 2006.
- [6] X. Wang, W. Freitas, and W. Xu, "Dynamic non-detection zones of positive feedback anti-islanding methods for inverter-based distributed generators," *IEEE Trans. Power Delivery*, vol. 26, pp. 1145-1155, 2011.
- [7] H. H. Zeineldin, "A-Droop Curve for Facilitating Islanding Detection of Inverter-Based Distributed Generation," *IEEE Trans. Power Electronics*, vol. 24, pp. 665-673, 2009.
- [8] Y. Jin, Q. Song, and W. Liu, "Anti-islanding protection for distributed generation systems based on reactive power drift," in 35th Annual Conference of IEEE Industrial Electronics (IECON 2009), 2009, pp. 3970-3975.
- [9] H. Zeineldin and S. Kennedy, "Sandia frequency-shift parameter selection to eliminate nondetection zones," *IEEE Trans. Power Delivery*, vol. 24, pp. 486-487, 2009.